Development of an instrumented model pile

Lundberg, AB; Broere, Wout; Dijkstra, J.

DOI
10.1201/9780429438660-42

Publication date
2018

Document Version
Final published version

Published in
Physical Modelling in Geotechnics

Physical Modelling in Geotechnics – McNamara et al. (Eds)
© 2018 Taylor & Francis Group, London, ISBN 978-1-138-34419-8

New method for full field measurement of pore water pressures

M. Ottolini
Technology Department, Heerema Marine Contractors SE, Leiden, The Netherlands

W. Broere
Geo-engineering Section, Delft University of Technology, Delft, The Netherlands

J. Dijkstra
Division of Geology & Geotechnics, Chalmers University of Technology, Gothenburg, Sweden

ABSTRACT: A cost effective method to measure pore water pressures in mixed granular media is described using 40 miniature MEMS pore pressure transducers. High accuracy in a single point is exchanged for lower accuracy full field measurements adjacent to the strongbox wall. The system is easily de-aired and calibrated due to the fact that the transducers are installed inside the strongbox wall. Additionally, the proof of concept test shows that the transducers are sufficiently accurate for problems with large pressure difference such as consolidation of clay while being subjected to elevated stress levels in the geotechnical centrifuge.

1 INTRODUCTION

In geotechnical engineering effort is made in quantifying the continuum stresses in granular media such as clays and sands. These exist out of three phases; particles in the solid phase leave pores in which water in the liquid phase and air in the gas phase is held. Experiments are often executed in a geotechnical centrifuge in order to satisfy similitude for the stress within these materials (Garnier et al. 2007). The acceleration of the centrifuge results into an increase of gravitational acceleration and therefore higher stress levels in the granular medium. These experiments require a strongbox to retain the soil. More conventional (miniature) pore pressure transducers, embedded in the soil or placed on the wall, are used where typically a high accuracy at a single point in space is required. Measurement of contact stress and pore pressures without influencing the soil state, especially the stiffness, around the sensor is not trivial (Talesnick 2005, Talesnick et al. 2014). Similar effects are observed for pore pressure transducers (Kutter, Sathialingam, & Herrmann 1990) or tensiometer design (Tarantino and Mongiovì 2002, Take and Bolton 2003), though most issues relate to the response time of the sensor for sensing dynamic events and stable operation at elevated stress levels and maintaining saturation in tensiometers. Traditionally, the Druck PDCR-81 is employed in physical model testing, however after its retirement alternatives are suggested (Stringer et al. 2014). Additional negative side effects of embedding transducers with their cables (Foray et al. , Jardine et al. 2013) in the specimen cannot be prevented. Also, the relatively high cost and/or large size of these transducers prohibit capturing the full spatial field. Recent developments in tactile sensing allow measurement of the contact load in a dense two-dimensional grid of points (Paikowsky and Hajduk 1997, Palmer et al. 2009). These promising sensors are, however, not easily converted for sensing pore water pressures in a soil sample and although the sensing element itself is inexpensive the data acquisition is not.

With the on-going developments in Micro Electro Mechanical System (MEMS) single chip solutions for sensing applications (Tanaka 2007, Tadigadapa and Mateti 2009) the instrumentation possibilities for geotechnical applications increase rapidly. MEMS accelerometers are already in use in the physical modelling community, e.g. Stringer et al. (2010). This paper, on the other hand, will introduce the use of cost effective MEMS pressure sensors (Eaton and Smith 1997) to acquire full field data of pore water pressures in soil samples adjacent to the wall in a strongbox. In principle the instrumentation is also applicable to measure the fluid phase in other mixed media.

2 EXPERIMENTAL SETUP

2.1 *Design objectives*

The MEMS pore pressure array (PPA) has primarily been developed for the TU Delft geotechnical centrifuge (Allersma 1994). This small beam centrifuge with a radius of 1.22 m has recently been re-equipped with modern data acquisition and camera facilities. The flight computer with wireless link, data acquisition and actuator control are all hosted on the central beam of the centrifuge. An embedded solution for data-acquisition near or in the sensor was preferred rather than developing a general robust miniature wireless data-acquisition system that interfaces conventional passive sensors (Gaudin et al. 2009), as the number of analog acquisition and amplifier channels is limited to 16. Furthermore, the setup should be autonomous from the centrifuge system, such that a similar setup could be quickly employed or cloned for instrumentation of 1-g physical model tests elsewhere in the laboratory and in long running autonomous in-situ tests. Finally, long-term stability and temperature compensation was deemed more important than dynamic response time as the primary motivation was to look into consolidation effects in clay resulting from installation of foundation elements.

2.2 *Sensor selection and application*

As opposed to MEMS accelerometers and gyroscopes, MEMS pressure transducers are more difficult to source, especially when considering the required (low) limit pressures and a sensing membrane that is insensitive to fluids. Finally, the Sensonor SP100 series transducers proved to be the best candidate for prototyping (Sensonor 2009). These pressure transducers are widely used for measurement of tire pressures in the automotive industry. Additionally to a sensing element these have a local embedded amplifier, 8 bit Analog to Digital Conversion (ADC), temperature and supply voltage sensing, and a digital communication interface (Serial Peripheral Interface: SPI). The triple stack glass-silicon-glass sensor element makes it suitable for wet environments such as saturated granular materials, as all instrumentation is encapsulated (Grelland 2001). Three different model types of the SP100 series have been used, the 1T (100 kPa), 2T (200 kPa) and 7T (700 kPa), to have a higher accuracy at the top part of the strongbox where lower pressures are expected. The stated resolution is 0.36 kPa for the 1T up to 1.25 kPa for the 7T model whilst the accuracy is 2% full scale. The latter is about 10 times worse than the PDCR-81 at 1/100th of the price. The surface mount packaging of the chip allows for a small centre-to-centre spacing. A hole in the top of the packaging allows for the fluid pressure to reach the sensing element. Isolation of the remainder of the chip from the soil and any harsh environment makes this solution more suitable for on wall measurements than embedment in the soil sample.

In the adopted application the MEMS transducers have been directly bonded to the aluminium wall of the strongbox. Contact between the water in the soil and the transducer is through a small channel in the wall with a 3 mm diameter at the transducer side and 5 mm diameter at the soil side. A sintered glass porous disc, of 5 mm diameter, prevents the soil from entering the channel. The channel and the porous disc are de-aired with silicon oil under a vacuum of -90 kPa to ensure a fast response of the transducer. Epoxy adhesive bonds the pressure transducers at the wall and

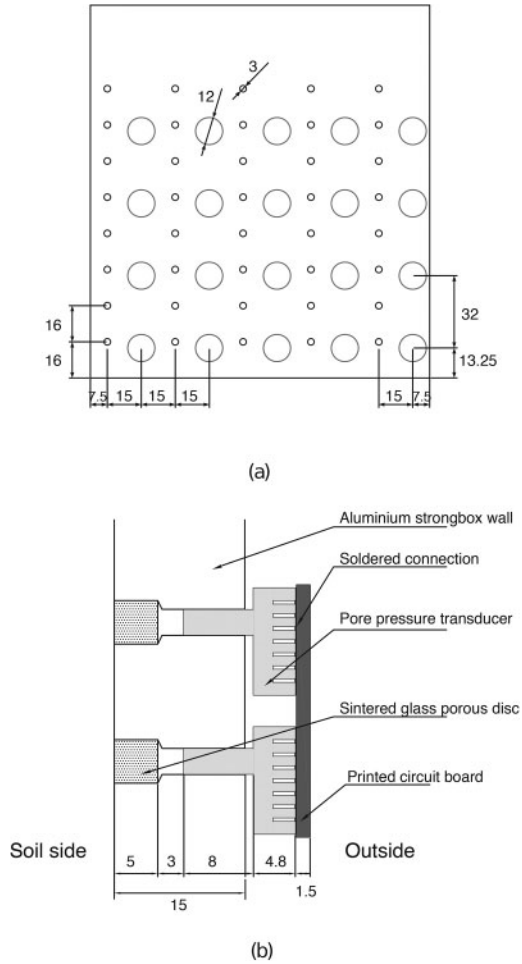

Figure 1. Design of pore pressure array (PPA); 1a: Mechanical drawing of PPA (measures in mm). 1b: Detailed mounting of MEMS package to sidewall.

ensures a watertight connection. The transducers have been spaced 30 mm horizontally and 16 mm vertically, in 8 rows of 5. A total of 40 transducers are placed to have sufficient field information. As a result the vertical spatial resolution is higher than the horizontal. The 14 pins sensor packages are soldered to a custom designed printed circuit board (PCB). The PCBs are a four-layer design consisting of a back and a front layer for placement of the electrical components and two inner planes serving as ground plane. Ten pore pressure transducers are combined on one sub-PCB and linked with a dedicated SPI BUS to the microcontroller. A technical drawing of the mechanical lay-out is shown in Figure 1.

2.3 *Data acquisition*

A functional block diagram of the electronic systems in the PPA is shown in Figure 2. The diagram is divided in three parts; the instrumentation on the wall itself,

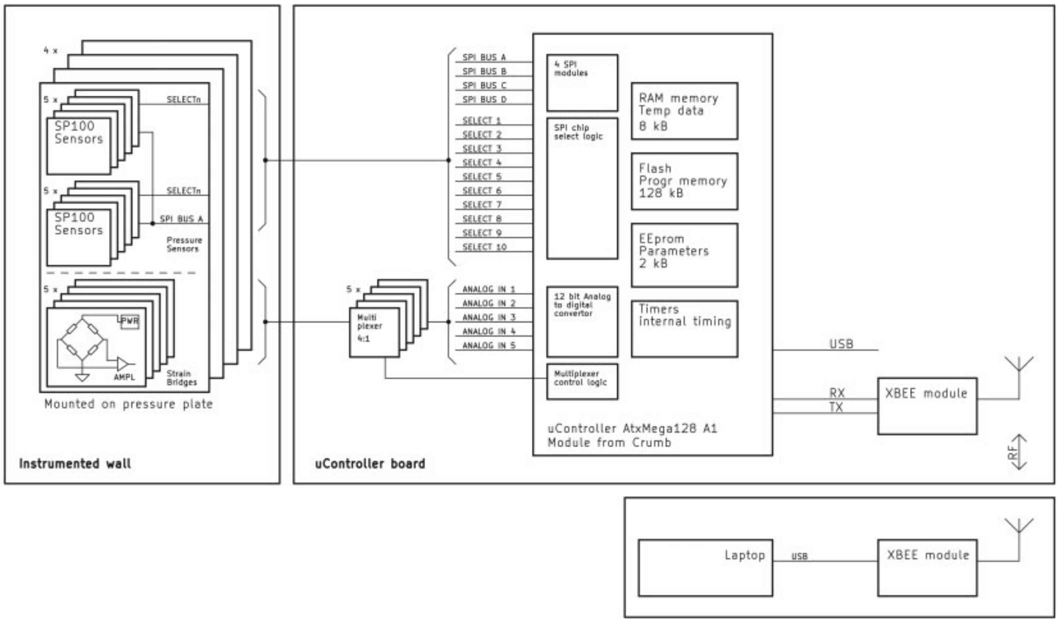

Figure 2. Functional block diagram of the electronic systems of the pore pressure array.

the data acquisition and transfer instrumentation and the data storage.

The data of each sub-PCB is connected through flat cables to a central CRUMBX microcontroller board (chip45 GmbH & Co. KG) that houses an Atmel AtxMega128 microcontroller. The availability of four SPI channels and 78 Programmable I/O Lines makes the microcontroller suitable for data acquisition of multiple channels on multiple PCBs. The flash drive of the CRUMBX is loaded with a control programme, written in C++, which handles the multiple channels retrieved. Ten I/O Lines are used as chip select lines. One transducer per PCB is selected and initialised simultaneously with the chip select line. The transducers are subsequently read and send to the microcontroller over a separate SPI bus, one for each PCB. This process is repeated until all pore pressure transducers are read. All the data is locally buffered until finishing reading the last sensor of the sequence. Subsequently, in sequences of 10 channels the data is wirelessly sent to a personal computer over a wireless connection through an XBee pro 60 mW wire antenna (Digi International Inc.). The latter acts as a wireless serial port at a baud rate of 115600 bps. Sampling of all transducers was set at a 1 second interval, though a real world upper sampling limit of 100 Hz can be reached. After reception the data is further handled in the custom written acquisition software developed at TU Delft, before being time stamped and saved to the hard drive.

The four sub-PCBs are equipped with the possibility to be used for strain gauge amplification with an Analog Devices AD8227 rail-to-rail output instrumentation amplifier and offset regulation of the strain gauges with a 500Ω potentiometer. On the data acquisition board five AD704 CMOS low voltage analog multiplexers are available to multiplex the data to the analog input channel of the microcontroller. The microcontroller is equipped with the necessary multiplexer control logic.

3 RESULTS

3.1 *Calibration*

The strongbox is modified to accommodate simultaneous saturation and calibration of all sensors. An aluminium lid equipped with two gas interconnectors seals the strongbox on the topside with a flat gasket inbetween the sidewalls and the lid. First the strongbox is filled with silicon oil and the air is evacuated under a vacuum to saturate the porous disc and cavity to the sensing membrane. Subsequently, the strongbox is filled with water and compressed air is used to calibrate the sensors in this temporary pressure vessel. The air compressor and regulator valve are too crude for accurate pressure readings, hence the second connector is attached to an analog precision manometer (accuracy <0.3 kPa) for measurement of the fluid pressure inside the strongbox. All the pore pressure transducers are simultaneously calibrated by applying pressure from 0 to 100 kPa in increments of 10 kPa. After stabilisation of the pressure, an average of 5 samples is taken from each transducer. A linear regression of the data is used to derive the calibration factor for further testing. Loading and reloading cycles have been applied to incorporate effects of hysteresis. The calibration is performed at room temperature (20°C $\pm$ 1°C) which is similar to the temperature in the

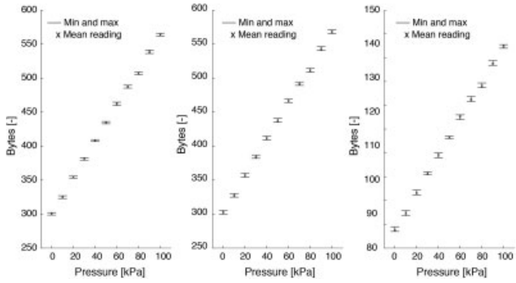

Figure 3. Calibration results for loading unloading loop of the MEMS pore pressure transducers with different pressure ranges (left: 100 kPa; middle: 200 kPa; right: 700 kPa. The mean, minimum and maximum readings of 10 sensors each have been plotted.

intended test. However, the readings can be corrected with the embedded temperature readings. Calibration results are shown in Figure 3 for the SP100-1T (left hand side), the SP100-2T (middle) and SP100-7T (right hand side) pressure is plotted against the raw sensor output in bytes. Minimum and maximum reading as well as the mean value are shown for 10 transducers of each type. The sensors are absolute pressure transducers, hence the intercept with the y-axis in the readings. Also, the limited calibration range for the 7T is due to the simultaneous calibration of all sensors with different maximum range. The calibration results indicate that in their new application the pressure sensors are operating within their rated specification of $\pm$ 2% full scale.

3.2 *Proof of concept N-g test*

The strongbox equipped with the PPA on one of the sidewalls has been used to monitor the pore pressure dissipation during consolidation of a kaolin soil specimen during self-weight consolidation in a geotechnical centrifuge. The standard procedure at TU Delft is that the kaolin clay powder is first mixed with de-aired water into slurry with high water content (>10 times the liquid limit). The strongbox used in the experiment has transparent windows made out of Plexiglas on the front and the back of the box and inner dimensions $(L \times W \times H)$ $180 \times 155 \times 150\,\mathrm{mm}^3$ one side wall is equipped with the PPA. Before the slurry is poured in the strongbox, all walls are sprayed with PTFE spray to reduce wall friction. Subsequently the slurry is consolidated into a solid sample using the TU Delft beam centrifuge at an acceleration level of 100-g. In Figure 4 a typical result of the full field pore pressure evolution during consolidation is shown, for three distinct prototype times: 45 days, 449 days and 898 days (t_{45}, t_{449}, t_{898}). The vertical axis is exaggerated for clarity. The measurements clearly indicate dissipation of pore-water pressure over time during self-weight consolidation. The difference pressure between sensors on the same depth stems from the eccentric placement of the strongbox in the centrifuge and the coriolis resulting from the rather short beam radius (Taylor 1995).

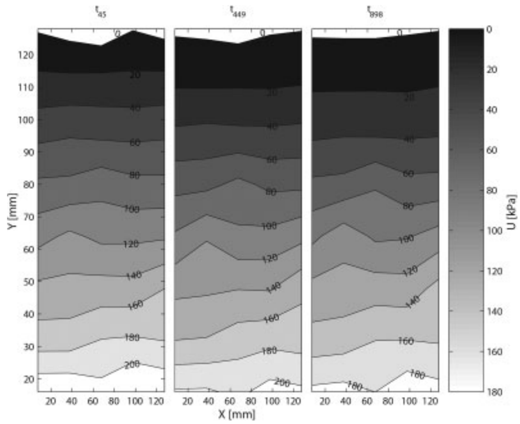

Figure 4. Full field measurement of dissipation of pore pressures due to self-weight consolidation of kaolin clay in a geotechnical centrifuge at 100-g after respectively 45 days (t_{45}), 449 days (t_{449}) and 898 days (t_{898}).

4 CONCLUSIONS

Only minor modifications are required to construct a cost effective pore pressure array (PPA) with a high number of sensors (40) using miniature MEMS pore pressure transducers. On-chip data acquisition allows for easy electrical interfacing to a micro-controller and subsequent wireless data transmission to any arbitrary receiver. High accuracy in a single point is exchanged for somewhat lower accuracy full field measurements adjacent to the strongbox wall. Due to the fact that the 40 pore pressure transducers are installed inside the wall they can be simultaneously de-aired and calibrated and additional detrimental effects from cables are prevented. The calibration of a large number of transducers corroborate that the sensors operate within their rated specifications ($\pm$ 2% full scale) as well as that the proof of concept test shows that the sensors continue to function well at elevated stress levels in the geotechnical centrifuge. Unique full field data can be gathered on both deformations and pore pressure response in the sample when the PPA is combined with full field deformation measurements on an adjacent transparent wall.

ACKNOWLEDGMENTS

The authors would like to express their gratitude to C. van Beek, J.J. de Visser, R. van Leeuwen and M. van der Meer for their assistance during the design and construction of the setup.

REFERENCES

Allersma, H. (1994). The university of delft geotechnical centrifuge. In *Proceedings International Conference Centrifuge 94*, pp. 47–52.

Eaton, W. & J. Smith (1997). Micromachined pressure sensors: review and recent developments. *Smart Materials and Structures 6*(5), 530.

Foray, P., J. Colliat, & J. Nauroy. Bearing capacity of driven model piles in dense sands from calibration chamber tests. In *Offshore Technology Conference*, pp. OTC–7194–MS.

Garnier, J., C. Gaudin, S. M. Springman, P. J. Culligan, D. J. Goodings, D. Konig, B. Kutter, R. Philips, M. Randolph, & L. Thorel (2007). Catalogue of scaling laws and similitude questions in geotechnical centrifuge modelling. *International Journal of Physical Modelling in Geotechnics 7*(3), 1–23.

Gaudin, C., D. White, N. Boylan, J. Breen, T. Brown, S. De Catania, & P. Hortin (2009). A wireless high-speed data acquisition system for geotechnical centrifuge model testing. *Measurement Science and Technology 20*(9), 095709.

Grelland, R. (2001). Tyre pressure monitoring microsystems. *Advanced Microsystems for Automotive Applications 2001*, 245–251.

Jardine, R., B. Zhu, P. Foray, & Z. Yang (2013). Interpretation of stress measurements made around closed-ended displacement piles in sand. *Géotechnique 63*(8), 613–627.

Kutter, B., N. Sathialingam, & L. Herrmann (1990). Effects of arching on response time of miniature pore pressure transducer in clay. *Geotechnical Testing Journal 13*(3), 164–178.

Paikowsky, S. & E. Hajduk (1997). Calibration and use of grid-based tactile pressure sensors in granular material. *Geotechnical Testing Journal 20*(2), 218–241.

Palmer, M., T. ORourke, N. Olson, T. Abdoun, D. Ha, & M. ORourke (2009). Tactile pressure sensors for soil-structure interaction assessment. *Journal of geotechnical and geoenvironmental engineering 135*(11), 1638–1645.

Sensonor (2009). *Sp100 compensated pressure sensors*. datasheet.

Stringer, M., J. Allmond, C. Proto, D. Wilson, & B. Kutter (2014). Evaluating the response of new pore pressure transducers for use in dynamic centrifuge tests. In *Proceedings of the 8th International Conference on Physical Modelling in Geotechnics*, Volume 1, pp. 345–351.

Stringer, M., C. Heron, & S. Madabhushi (2010). Experience using mems-based accelerometers in dynamic testing. In *Proceedings of the 7th International Conference on Physical Modelling in Geotechnics*, Volume 1, pp. 389–394.

Tadigadapa, S. & K. Mateti (2009). Piezoelectric mems sensors: state-of-the-art and perspectives. *Measurement Science and technology 20*(9), 092001.

Take, W. & M. Bolton (2003). Tensiometer saturation and the reliable measurement of soil suction. *Géotechnique 53*(2), 159–172.

Talesnick, M. (2005). Measuring soil contact pressure on a solid boundary and quantifying soil arching. *Geotechnical Testing Journal 28*(2), 1–9.

Talesnick, M., M. Ringel, & R. Avraham (2014). Measurement of contact soil pressure in physical modelling of soil–structure interaction. *International Journal of Physical Modelling in Geotechnics 14*(1), 3–12.

Tanaka, M. (2007). An industrial and applied review of new mems devices features. *Microelectronic engineering 84*(5), 1341–1344.

Tarantino, A. & L. Mongiovì (2002). Design and construction of a tensiometer for direct measurement of matric suction. In *Proceedings of the 3nd International Conference on Unsaturated Soils, Recife, Brazil*, Volume 3, pp. 319–324.

Taylor, R. (1995). Centrifuges in modelling: principles and scale effects. *Geotechnical centrifuge technology*, 19–33.